Available online at www.sciencedirect.com
SCIENCE DIRECT
Journal of Solid State Chemistry 179 (2006) 2458–2465
JOURNAL OF SOLID STATE CHEMISTRY
www.elsevier.com/locate/jssc

Selective substitution of vanadium for molybdenum in $Sr_2(Fe_{1-x}V_x)MoO_6$ double perovskites

Q. Zhang[a], G.H. Rao[a,*], Q. Huang[b], X.M. Feng[c], Z.W. Ouyang[a], G.Y. Liu[a], B.H. Toby[b], J.K. Liang[a]

[a]*Beijing National Laboratory for Condensed Matter Physics, Institute of Physics, Chinese Academy of Sciences, Beijing 100080, People's Republic of China*
[b]*NIST Center for Neutron Research, National Institute of Standards and Technology, Gaithersburg, MD 20899-8562, USA*
[c]*Institute of Materials Science and Technology, Nanjing University of Aeronautics and Astronautics, Nanjing 210016, People's Republic of China*

Received 13 March 2006; received in revised form 30 April 2006; accepted 2 May 2006
Available online 6 May 2006

Abstract

The crystal and magnetic structures of $Sr_2(Fe_{1-x}V_x)MoO_6$ ($0.03 \leqslant x \leqslant 0.1$) compounds are refined by alternately using X-ray powder diffraction (XRD) and neutron powder diffraction (NPD) data collected at room temperature. The refinement results reveal that the V atoms selectively occupy the Mo sites instead of the Fe sites for $x \leqslant 0.1$. The *3d*/*4d* cation ordering decreases with the increase of the V content. Slight distortions in the lattice and metal octahedra are shown at 300 K, and the distortions increase at 4 K. The magnetic structure at 4 K can be modeled equally well with the moments aligning along [001], [110] or [111] directions. The total moments derived from the NPD data for the [110] and [111] direction models agree well with the magnetic measurements, whereas the [001] model leads to a smaller total moment. Bond valence analysis indicates that Sr ions are properly located in the structure and Mo ions are compatible with both the Fe sites and the Mo sites. The electronic effects are suggested to be responsible for the selective occupation of the V on the Mo sites due to the different distortions of the FeO_6 and MoO_6 octahedra.

Keywords: Crystal and magnetic structures; Preferential site occupation; Neutron powder diffraction; Double perovskites

1. Introduction

The ordered double perovskite compound Sr_2FeMoO_6 has received considerable attention in recent years owing to its appreciable room temperature low-field magnetoresistance (LFMR) that offers potential applications in spintronic devices and is of fundamental interest in condensed matter physics. Electronic structure calculations and optical spectroscopy investigations indicate that Sr_2FeMoO_6 is of half-metallic nature, i.e., the majority spin band is gapped and occupied essentially by the $3d^5$ up-spin electrons of Fe^{3+} ions, while the conduction band is occupied by both the Mo 4*d* t_{2g} and the Fe 3*d* t_{2g} down-spin electrons, leading to a full polarization of the itinerant carriers [1–3]. Both the ferrimagnetic coupling between the magnetic moments of the Fe and the Mo sublattices and the metallic conductivity are considered to be induced via itinerant down-spin electrons [2]. The observed LFMR in Sr_2FeMoO_6 can be attributed to a tunneling of the spin-polarized carriers across grain/domain boundaries [4].

An ideal ordered Sr_2FeMoO_6 consists of corner-sharing FeO_6 and MoO_6 octahedra alternately arranged along all three directions with the voids among the octahedra being filled by larger Sr ions. Therefore, Fe and Mo atoms form a rock-salt structure (rock-salt ordering). If one considers a spin-only contribution of 5 Bohr magneton per formula unit (μ_B/f.u.) of the Fe sublattice and 1 μ_B/f.u. of the Mo sublattice, a saturation moment of 4 μ_B/f.u. is anticipated for an ideally ordered Sr_2FeMoO_6 within the framework of the simplest ferrimagnetic arrangement model (the FIM model), which assumes that the Fe and Mo sublattices couple antiferromagnetically [5]. However, magnetic measurements and crystal structure analysis indicate that Sr_2FeMoO_6 is not perfectly ordered due to intrinsic antisite defects (AS), i.e., small numbers of Fe and Mo atoms

*Corresponding author. Fax: +86 10 8264 9531.
E-mail address: ghrao@aphy.iphy.ac.cn (G.H. Rao).

0022-4596/$ - see front matter © 2006 Elsevier Inc. All rights reserved.
doi:10.1016/j.jssc.2006.05.001

exchange sites. This can happen because the valence difference and ionic radius difference between Fe^{3+} and Mo^{5+} fall in the region where ordered and disordered double perovskites can coexist [6]. Both experiments and computer simulation have showed that the LFMR and the saturation moment of Sr_2FeMoO_6 are sensitive to the presence of the AS [5,7,8]. Substitutions of W for Mo [9,10], Cu for Fe [11], and Mn for Fe [12] reduced the AS content. In contrast, substitutions of Cr or V for Fe increased the AS content (i.e. the Mo content on the Fe site) in $Sr_2Fe_{1-x}T_xMoO_6$ (T = Cr, V) [13,14]. For $Sr_2Fe_{1-x}Cr_xMoO_6$ ($x = 1/4$, $1/2$, $3/4$ and 1.0), neutron diffraction revealed that Cr preferentially occupied the Mo sites and, interestingly, the population ratio of Cr on the Fe sites to the Cr on the Mo sites was approximately a constant ($\approx$1:2) for $x = 0.25-1.0$ [13]. Oxygen deficiency was detected for the Cr content greater than 0.25. Ritter et al. investigated the structure of a series of 3*d*-metal doped $Sr_2Fe_{3/4}T_{1/4}MoO_6$ (T = Sc, Ti, V, Cr, Mn, Fe, Co) by X-ray powder diffraction (XRD) and neutron powder diffraction (NPD) [15]. The dopant T distributed unevenly on the Fe and the Mo sites, while a preferential occupation of T on the Fe sites was observed, except for T = Cr. The size and valence state of the dopant are considered to affect the relative distribution of T on the Fe and Mo sites. In comparison to the parent compound Sr_2FeMoO_6 with AS = 0.05, the T-doping increased the Mo content on the Fe sites (AS), i.e. reduced the 3*d*/4*d* cation ordering.

Since the LFMR and the saturation moment of Sr_2FeMoO_6 are sensitive to the presence of the AS [5,7,8], detailed information on structure stability, atomic occupancies, cation ordering and magnetic structure is indispensable for understanding the physics of the LFMR of the double perovskite compounds. Many neutron diffraction studies have been carried out on parent compound Sr_2FeMoO_6 [15–18] and heavily doped $Sr_2(Fe_{1-x}T_x)MoO_6$ ($x \geqslant 0.25$) [13,15]. However, similar work on lightly doped compounds is less reported in literature. The relatively light doping provides an opportunity to examine the perturbation of the doping to the stability and physical properties of the double perovskite compounds.

The crystal structure, electrical transport and magnetic properties of the lightly V-doped $Sr_2(Fe_{1-x}V_x)MoO_6$ compounds ($0 \leqslant x \leqslant 0.1$) have been reported previously [14]. Based on X-ray diffraction, it was revealed that the 3*d*/4*d* cation ordering decreased with the V content. Because of the tiny difference in X-ray atomic scattering factor between Fe and V, the (Fe, V) was treated as a single entity and the occupancy of Mo on the Fe sites (= the occupancy of (Fe, V) on the Mo sites) was refined as the AS. The derived AS was greater than the V content, x, for all the investigated $Sr_2(Fe_{1-x}V_x)MoO_6$ ($0 \leqslant x \leqslant 0.1$). On the assumption that the V occupied exclusively the Mo sites, i.e. $Sr_2(Fe_{1-AS}Mo_{AS})(Mo_{1-AS}Fe_{AS-x}V_x)O_6$, the FIM model reasonably reproduced the experimental magnetic moments as a function of the V content. However, the assumed distribution of V in the investigated compounds is in contradistinction to the cases of the heavily doped $Sr_2Fe_{3/4}V_{1/4}MoO_6$ [15] and $Sr_2(Fe_{1-x}Cr_x)MoO_6$ ($x \geqslant 0.25$) [13]. In this paper, we combine XRD and NPD techniques to ascertain the distribution of Fe, Mo, and V cations in the lightly V-doped $Sr_2(Fe_{1-x}V_x)MoO_6$ compounds ($0 \leqslant x \leqslant 0.1$). In addition, magnetic structure of $Sr_2Fe_{0.9}V_{0.1}MoO_6$ at 4 K is modeled by considering different alignments of magnetic moments.

2. Experimental

The preparation of polycrystalline $Sr_2(Fe_{1-x}V_x)MoO_6$ ($0 \leqslant x \leqslant 0.1$) was described in detail previously [14]. The samples were synthesized by standard solid-state reactions at 1280 °C under a reduction atmosphere (flowing 5% H_2/Ar gas) with several intermediate grindings. XRD detected no impurity phases in the samples. The XRD was performed on a Rigaku D/max 2500 diffractometer with Cu$K\alpha$ radiation (50 kV × 250 mA) and a graphite monochromator for the diffracted beam in Bragg–Brentano geometry. The patterns were collected between $2\theta = 15°$ and 100° in a step of 0.02° with a sampling time of 1 s per step. The NPD experiments were performed at NIST Center for Neutron Research (NCNR) on the high-resolution, 32-counter BT-1 diffractometer with a monochromatic neutron beam of wavelength 1.5403(2) Å. Collimators with horizontal divergence of 15, 20, and 7 min of arc were used before and after the monochromator and after the sample, respectively. Data were collected in the 2θ range of 10–160° with a step of 0.05°. The crystal and magnetic structures were refined using the program FULLPROF [19].

3. Results

The crystal structure of the V-doped $Sr_2(Fe_{1-x}V_x)MoO_6$ was refined based on space group $I4/m$ as mostly reported for the parent compound Sr_2FeMoO_6 with the rock-salt ordering [13,16,20]. The space groups $I4/mmm$ [9] and $P4_2/m$ [17] have also been suggested for Sr_2FeMoO_6. These three space groups are in fact only slightly different in describing the symmetry of Sr_2FeMoO_6 and become equivalent, provided that some reasonable constraints on the position parameters of oxygen are applied [13].

It is well known that determination of the distribution of three different kinds of atoms (Fe, V, Mo) on two available crystallographic sites (2*a* and 2*b* in $I4/m$) requires, in principle, at least two sets of diffraction data with differing atomic cross sections that can provide two linearly independent structure factors [21] and even then is nontrivial by Rietveld refinement. Since it is difficult in practice to measure absolute intensities with precision, a scale factor is usually employed to convert arbitrary intensities to absolute intensities, which raised the number of data sets required to three. Though we have only two sets of diffraction data (XRD and NPD), we first intended

to perform a combined refinement of XRD and NPD data at 300 K. However, strong correlations (>90%) among the derived occupancies and temperature factors were observed in the combined refinements, probably due to the relatively small 2θ range of the XRD data [22]. In addition, the refinement result also varied with the weighting factors preset to each pattern. Thus, no conclusive results can be achieved from the combined refinements.

Fig. 1 compares the superstructure (011) peak arising from the $3d/4d$ ordering on XRD and NPD patterns at room temperature (the NPD data are shifted to high angle by 1° for clarity). The (011) peak in NPD also contains contribution from magnetic scattering, regardless of the cation ordering [18], whereas it results exclusively from the $3d/4d$ ordering in XRD. Obviously, the $3d/4d$ ordering is much better manifested in XRD than in NPD, i.e., the NPD is less sensitive to the $3d/4d$ ordering. Our recent computer simulation work seems to corroborate this point [23]. Based on the simulated XRD and NPD data with different preset antisite contents AS, ranging from 0% (completely ordered) to 50% (completely disordered), Rietveld refinements revealed that the AS could be reproduced satisfactorily from the refinement of XRD data with a relative deviation smaller than 4%, whereas the relative deviation of AS derived from the refinement of NPD data was much larger and could be as high as 50% for low value of AS.

Therefore, the difference in X-ray scattering factor between $3d$ and $4d$ metals is large enough for locating the *3d* and *4d* metals in $Sr_2(Fe_{1-x}V_x)MoO_6$ by XRD, whereas the large difference in neutron scattering length between Fe and V ($\sigma = 9.45$, -0.3824, 6.715, 7.02, and 5.803 fm for Fe, V, Mo, Sr, and O, respectively) enables us to locate Fe and V accurately by NPD. By alternately using of XRD and NPD data, it should be possible to locate the Fe, V, and Mo atoms on $2a$ (Fe sites) and $2b$ (Mo sites) in $Sr_2(Fe_{1-x}V_x)MoO_6$. Similar approach was adopted for the refinements of $Sr_2(Fe, T)MoO_6$ compounds [13,15] and Sr_2FeMoO_6 [18]. The details of the refinements are as follows.

First, we refined the crystal structure using the XRD data collected at room temperature by assuming the nominal stoichiometry of $Sr_2(Fe_{1-x}V_x)MoO_6$, treating Fe and V as a single entity and fixing the temperature factors of the atoms to the values of Sr_2FeMoO_6 derived from NPD by Chmaissem et al. [16]. The AS content, i.e., $4d$ metal (Mo) on the Fe sites ($=3d$ metal on the Mo sites), was satisfactorily derived as we reported previously [14]. Then, we fixed the occupancies of Mo on the Fe sites and on the Mo sites (AS and 1−AS, respectively) and refined the crystal structure by using the NPD data at 300 K in the 2θ range of 40–160°. Since the magnetic contribution at 300 K to NPD is negligible for $2\theta > 40°$ [13], the NPD in this 2θ range results essentially from nuclear scattering. The occupancies of Fe and V on the Fe and the Mo sites and the oxygen site occupancies, together with position parameters, profile parameters and temperature factors, were refined. The refinement result showed that the occupancy of V on the Fe sites was negative and the stoichiometry of oxygen was close to 6 with a deviation smaller than 1% for all compounds investigated ($0.03 \leqslant x \leqslant 0.1$). Oxygen deficiency was also not observed in the refinement results of Ref. [15] for $Sr_2Fe_{0.75}V_{0.25}MoO_6$ and of Ref. [16] for Sr_2FeMoO_6. Therefore, we assigned the V occupancy to occur exclusively on the Mo sites as we suggested based on magnetic measurements and FIM model [14]. Setting the occupancy of V on the Fe sites to zero, i.e., $Fe_{1-AS}Mo_{AS}$ on the Fe sites and $Mo_{1-AS}Fe_{AS-x}V_x$ on the Mo sites with the AS derived from XRD, and fixing the oxygen stoichiometry to six per

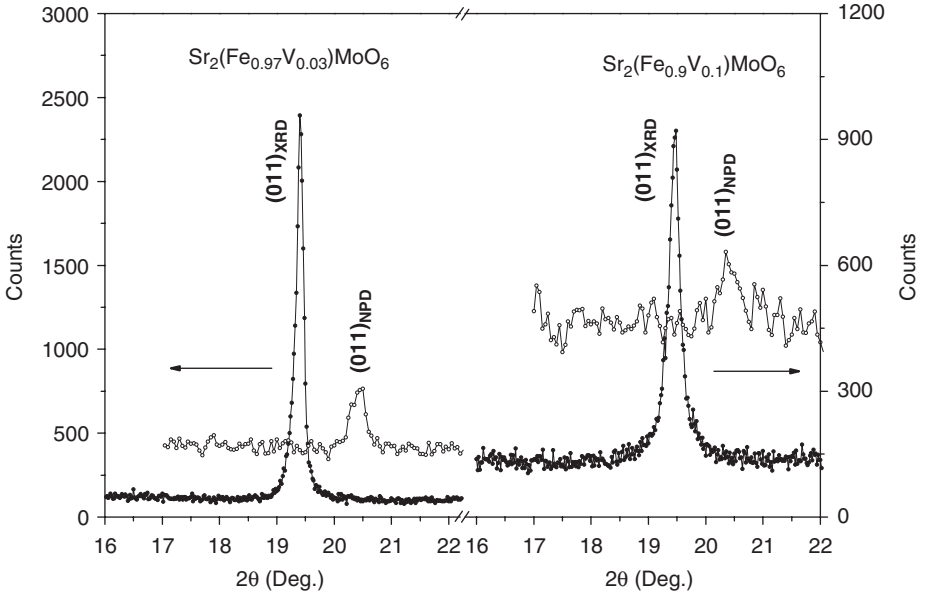

Fig. 1. Comparison of the superstructure (011) peak in XRD and NPD at room temperature. The NPD data are shifted to higher angle by 1°.

formula, one more refinement was performed in order to derive thermal parameters of the atoms and the V content on the Mo sites. The stoichiometry of Sr is not refined and is fixed to two, which was demonstrated by the refinement of Ritter et al. for $Sr_2Fe_{0.75}V_{0.25}MoO_6$ [15] and is confirmed by bond valence analysis discussed below.

Using the temperature factors derived from present refinement of the NPD data for $Sr_2Fe_{1-x}V_xMoO_6$, we repeated the refinement of crystal structure based on the XRD data. A new set of AS was derived, which agrees with our previous report in Ref. [14] within 2%. The occupancies of V on the Fe and Mo sites and oxygen stoichiometry were checked again using the NPD data at 300 K as described above. The same conclusion was derived. In the final refinement, the occupancy and stoichiometry of the compounds were treated as $Sr_2(Fe_{1-AS}Mo_{AS})(Mo_{1-AS}Fe_{AS-x}V_x)O_6$. Except that the AS was fixed to the value derived from the XRD data in present work, the V content on the Mo sites (x) and temperature factors of each sites were treated as refinable parameters in fitting the NPD data. At this stage, the magnetic contribution was also included and accordingly the full NPD pattern in the 2θ range of 10–160° was used. The moments of the Fe and the Mo were presumed to have a collinear arrangement as discussed below. The fitting to the NPD profile and the expected Bragg positions are exemplied on the upper panel of Fig. 2 for $Sr_2Fe_{0.9}V_{0.1}MoO_6$ at 300 K. (The inset shows the XRD data around $2\theta = 76.4°$ with the $K_{\alpha 2}$ contribution being stripped, which manifests three reflections of the space group $I4/m$.) Since the perovskite unit cell has already been doubled by the $3d/4d$ ordering, all the magnetic reflection positions are coincident with the nuclear Bragg reflection positions. Satisfactory fitting to the NPD data at 300 K is achieved

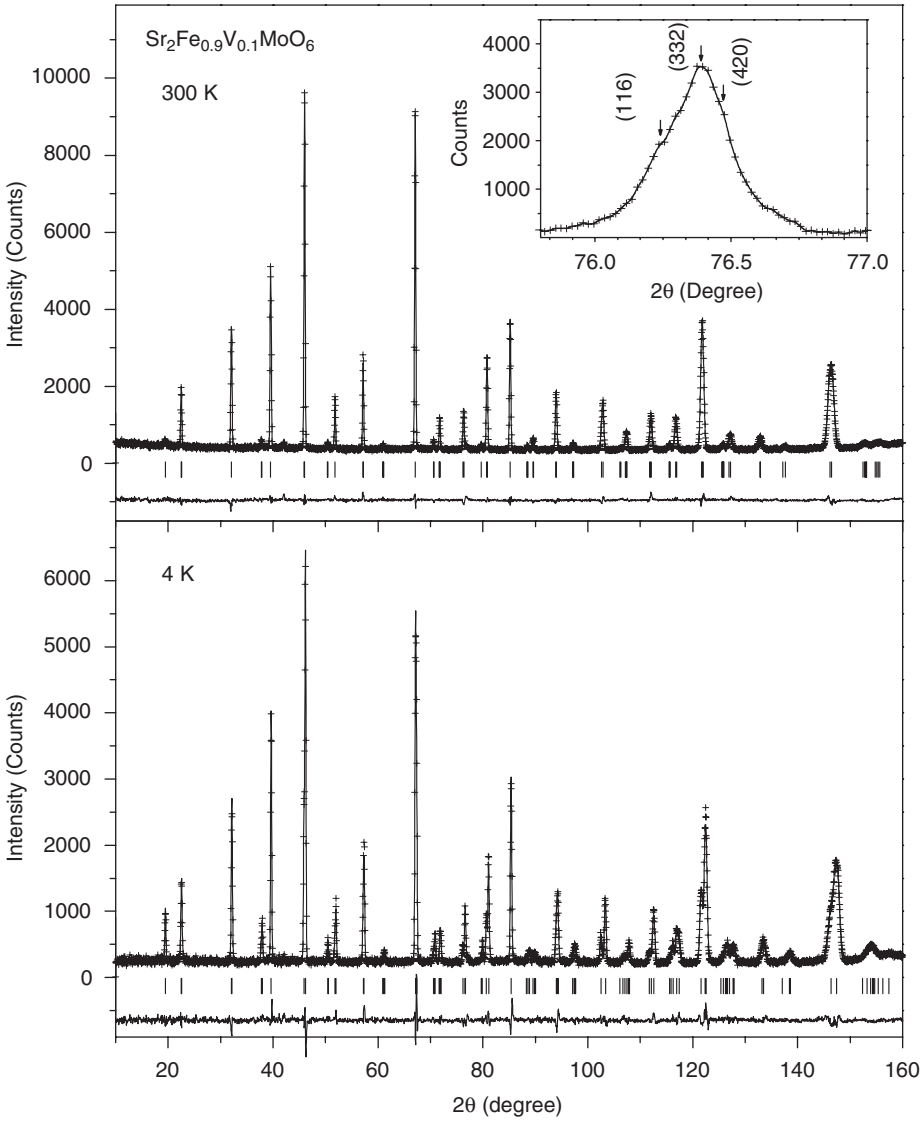

Fig. 2. Observed (crosses) and calculated (solid line) NPD patterns of $Sr_2Fe_{0.9}V_{0.1}MoO_6$ at 300 K (upper) and 4 K (lower). The vertical lines indicate the Bragg reflection positions for both the nuclear and the magnetic scattering. The difference between the observed and the calculated intensities is shown at the bottom of the figure. The inset in upper panel shows the XRD data around $2\theta = 76.4°$ with the $K_{\alpha 2}$ contribution being stripped.

Table 1
Structural parameters for $Sr_2(Fe_{1-x}V_x)MoO_6$

Compound Temperature	$Sr_2Fe_{0.97}V_{0.03}MoO_6$ 300 K	$Sr_2Fe_{0.95}V_{0.05}MoO_6$ 300 K	$Sr_2Fe_{0.92}V_{0.08}MoO_6$ 300 K	$Sr_2Fe_{0.90}V_{0.10}MoO_6$ 300 K	$Sr_2Fe_{0.90}V_{0.10}MoO_6$ 4 K
a (Å)	5.57197(2)	5.57243(2)	5.57187(2)	5.57085(2)	5.55369(2)
c (Å)	7.89912(4)	7.89659(5)	7.89431(6)	7.89239(6)	7.89926(5)
$\sqrt{2}a/c$	0.9976	0.9980	0.9982	0.9982	0.9943
V (Å^3)	245.242(1)	245.205(2)	245.084(2)	244.935(2)	243.641(2)
Sr					
At (1/2, 0, 1/4)					
B (Å^2)	0.850(5)	0.916(5)	0.969(6)	0.930(6)	0.441(8)
Fe/Mo[a]					
At (0, 0, 0)	0.904(4)/0.096(4)	0.848(4)/0.152(4)	0.797(4)/0.203(4)	0.763(3)/0.237(3)	0.763(3)/0.237(3)
B (Å^2)	0.53(5)	0.78(6)	0.81(5)	0.78(5)	0.39(1)
μ (μ_B)	2.2(1)	1.8(2)	1.4(3)	0.5(0)	3.5(2)
Mo/Fe/V[b]					
At (0, 0, 1/2)	0.904(4)/0.040(3)/0.056(3)	0.848(4)/0.107(3)/0.045(3)	0.797(4)/0.120(3)/0.083(3)	0.763(3)/0.128(2)/0.109(2)	0.763(3)/0.128(2)/0.109(2)
B (Å^2)	0.11(5)	0.18(7)	0.11(6)	0.09(6)	0[c]
μ (μ_B)	−0.4(2)	−0.5(3)	−0.4(4)	0[c]	−0.7(2)
O(1)					
At (0, 0, z)					
z	0.2529(5)	0.2518(7)	0.2511(10)	0.2508(10)	0.2553(2)
B (Å^2)	0.968(18)	0.804(20)	0.933(23)	0.843(23)	0.702(9)
O(2)					
At (x, y, 0)					
x	0.2699(4)	0.2685(5)	0.2664(6)	0.2652(6)	0.2744(3)
y	0.2348(3)	0.2349(5)	0.2353(6)	0.2361(6)	0.2303(3)
B (Å^2)	1.028(10)	1.201(10)	1.157(11)	1.212(12)	0.476(16)
R_P (%)/R_{WP} (%)/χ^2	3.93/4.99/1.21	4.51/5.64/1.30	4.21/5.23/1.13	3.98/5.03/1.38	6.43/7.96/2.52

Space group: $I4/m$. Sr at $4d$(1/2, 0, 1/4), Fe/Mo at $2a$(0, 0, 0), Mo/Fe/V at $2b$(0, 0, 1/2), O(1) at $4e$(0, 0, z), and O(2) at $8h$(x, y, 0). Magnetic moments along [110] direction: $\mu_x = \mu_y$, $\mu_z = 0$. R_P and R_{WP} are residuals of fitting to the pattern and the weighted pattern, respectively. χ^2 is a "goodness of fit" indicator (Ref. [19]).

[a]Occupancies are derived from the refinement of XRD data and fixed in the refinement of the NPD data.

[b]The distribution of Fe and V on the Mo sites is derived from the NPD data by fixing the Mo occupancy as determined from the XRD data.

[c]Fixed value (see text).

for all the compounds investigated as indicated by the "goodness of fit", χ^2, listed in Table 1. The AS increases with the V content as reported in Ref. [14]. Except for the compound with the lowest V content ($x = 0.03$), the V content on the Mo sites derived from the NPD data is almost the same as the nominal V content, which justifies the refinement results. For the parent compound Sr_2FeMoO_6, small Fe deficiency or Mo deficiency were reported based on the NPD experiments [16,17], but no AS were detected in their work. Since about 10% antisite defect was derived from our XRD data for $x = 0.03$ and the Mo stoichiometry was fixed to 1.0, the slight Fe deficiency (i.e. the higher V content than the nominal one) occurring on the Mo sites in this work could be an artifact.

The crystal and magnetic structures of $Sr_2Fe_{0.9}V_{0.1}MoO_6$ at 4 K were refined based on exclusively the NPD data. Occupancies of atoms were fixed to those determined at 300 K. Considering that the thermal factor on the Mo sites is small at 300 K and should be reduced at low temperature, the thermal factor on the Mo sites is fixed as zero at 4 K. A collinear arrangement of the Fe and the Mo moments was assumed. Based on the Rietveld refinements of the NPD data, Chmaissem et al. derived that the moments were roughly along the [111] direction for Sr_2FeMoO_6 [16], whereas Ritter et al. found that the alignment of the moments along [110] gave the best fit to their NPD data [17] and Sánchez et al. fixed the moments to the [001] direction [18]. We tested all these three magnetic structure models with the moments aligning along [001], [110], and [111], respectively. The three models fit the NPD at 4 K equally well, as evidenced by almost the same "goodness of fit", χ^2, and by the visual inspection of the output plots. The refinement results show that the moments of Fe couple antiferromagnetically with the moments of Mo as expected and reported in many literatures for Sr_2FeMoO_6. The models with the moments along [110] or [111] result in almost the same total moments of the compound, 2.8(3) μ_B/f.u. for the [110] orientation and 2.7(3) μ_B/f.u. for the [111] orientation, which agree well with the saturation moment derived from magnetization measurement (2.67 μ_B/f.u. [14]). In contrast, the model with the moments along [001] gives a total moment of 2.2(3) μ_B/f.u. Because of the small tetragonal distortion ($\sqrt{2}a/c = 0.9943$ for $x = 0.1$), a unique determination of the direction of the moments in fact becomes rather difficult exclusively based on the NPD data. As an example, the refinement results with the [110] orientation model for the magnetic structure at 300 and 4 K are listed in Table 1. The observed and the calculated NPD patterns for $Sr_2Fe_{0.9}V_{0.1}MoO_6$ at 4 K are shown in the lower panel of Fig. 2.

It should be mentioned that the moments on the Fe sites and on the Mo sites are not constrained during the

refinements. They show a strong correlation (>85%), indicating that they are interdependent and cannot be determined uniquely by the unconstrained refinement [16], though the derived total moment of the compound agrees well with the experimental one. For the moment on the Mo sites, the derived value at 300 K can in fact be regarded as zero within the estimated standard deviation, and for $x = 0.1$ we had to set $\mu(\mathrm{Mo}) = 0$ to achieve the stable result. Nevertheless, the total moment of the compounds at 300 K shows a trend of decreasing with the V content, in consistence with the experimental observations [14].

4. Discussion

It is well known the cation arrangement on the *B* sites of a stoichiometric double perovskite is controlled by the charge difference and secondarily by the size difference of the *B* cations [6]. The rock salt arrangement is most common if the charge difference is greater than two, but the random arrangement is preferred if the charge difference is less than two. When the charge difference is two and the ionic radius difference is less than 0.2 Å, both the rock salt and the random arrangements can occur, depending on synthesis conditions. For Sr_2FeMoO_6, the nominal charge difference of the *B*-cations is two and the ionic radius difference is 0.035 Å ($r_{Fe^{3+}} = 0.645$ Å, $r_{Mo^{5+}} = 0.61$ Å, for CN = 6 [24]), which could be the cause for the happening of small amount of AS in the compound. Though the occurrence of the AS reduces both the difference in average charge and the difference in average size of the *B* cations between the Fe and the Mo sites, the configuration entropy due to the AS, which can be expressed as: $-2RT[\mathrm{AS}\ln\mathrm{AS} + (1-\mathrm{AS})\ln(1-\mathrm{AS})]$, could play a crucial role in stabilizing the ordered double perovskite structure, where AS is the antisite defect concentration as defined before, *R* is the gas constant and *T* is the temperature in Kelvin. This scenario coincides with the fact that the cationic ordering in Sr_2FeMoO_6 is progressively enhanced when raising the sintering temperature [3,5].

For slightly distorted perovskite structures, microdefects other than AS may take place. The presence of microtwins in $BaPbO_3$ was proposed based on very high-resolution time-of-flight NPD studies [25] and fine scale translational stacking faulting in A_2InNbO_6 (*A* = Ba, Sr) were revealed by deliberate profile analysis of the NPD data and transmission electron microscope investigation [26]. The existence of these microdefects can account for the anisotropic line broadening of the diffraction data. For A_2InNbO_6, the absence of AS could be attributed to the large difference in ionic radius between In^{3+} and Nb^{5+} (= 0.16 Å, $r_{In^{3+}} = 0.800$ Å, $r_{Nb^{5+}} = 0.64$ Å, for CN = 6 [24]). Based on the structural parameters derived from the antisite refinement of the NPD data for Ba_2InNbO_6 [26], the Global Instability Index R_1 as defined below is calculated to be as high as 0.38 valence units (v.u.), indicating the antisite structural model is likely unstable due to large residual bond strain in the structure induced by the AS [27]. In contrast, the ionic radius difference between Fe^{3+} and Mo^{5+} is very small for Sr_2FeMoO_6, the AS will not introduce significant residual bond strain in the structure. As discussed below, the R_1 for all the investigated $Sr_2(Fe_{1-x}V_x)MoO_6$ ($x \leqslant 0.1$) is well below 0.2 v.u., the empirical critical value for a stable structure. The close correlation between saturation moment and antisite concentration (AS) [5,7,8] suggests that the antisite structural model be reasonable for the Sr_2FeMoO_6-related double perovskites. Though the presence of the microdefects such as twins, stacking faults, etc., in Sr_2FeMoO_6-related compounds cannot be ruled out completely, the AS affects the magnetic properties and the LFMR of the compounds primarily, whereas the effects of other microdefects are secondary. The presence of AS defects, giving rise to substitution disorder and displacement disorder in Ref. [28], can also lead to the anisotropic broadening, shift and asymmetry of the peaks of diffraction data.

Since the ionic radii of Fe^{3+} and V^{3+} are almost the same ($r_{Fe^{3+}} = 0.645$ Å, $r_{V^{3+}} = 0.640$ Å, for CN = 6 [24]), neither the charge difference effect nor the size difference effect favors the selective occupation of V on the Mo sites in $Sr_2(Fe_{1-x}V_x)MoO_6$. Table 2 shows bond length between cations and oxygen and the bond valence sum [27] of each ion on different sites calculated from the crystallographic data at 300 K by program Bond-Str integrated to Fullprof_suite [19]. The good agreement between the bond valence sum of Sr and its chemical valence is indicative of the appropriate sites for the Sr ions in the structure. Likewise, the bond valence sums of Mo on both the Fe sites and the Mo sites are close to the chemical valence of Mo^{5+}, which implies that both the sites can accommodate themselves properly to the Mo^{5+} ions. The bond valence sums of Fe and V on the Fe sites are close to three and increase slightly with *x*, i.e. as the Mo content on Fe sites increases. However, the bond valence sum of the 3*d* cation on the Mo sites is obviously larger than three. The same feature is observed for the bond valence sum of Fe on the Mo sites in parent Sr_2FeMoO_6, based on the structural data derived from NPD [16,17] and single crystal XRD [3]. On both the Fe and the Mo sites, the bond valence sum of V is about 0.15 v.u. (valence unit) smaller than that of Fe, which leads to the bond valence sum of V on the Mo sites for $x = 0.03$ ($S = 3.39$ v.u.) to be comparable to that of Fe on the Fe sites for $x = 0.1$ ($S = 3.32$ v.u.). Therefore, for $x \leqslant 0.1$ the selective occupation of V on the Mo site would introduce smaller lattice strain than the case when the same amount of Mo sites was occupied by the Fe. It is not uncommon that in some isomorphous series of structures, certain sites are found to be consistently under- or overbonded, indicating the presence of tensile or compressive bond strain, respectively [27]. The stability of a structure can be conveniently measured by the Global Instability Index R_1, defined as the root-mean-square average of the difference between the bond valence sum and the chemical valence of each ion in a structure.

Table 2
Bond lengths and bond valence sum of the ions in $Sr_2(Fe_{1-x}V_x)MoO_6$

x	$x = 0.03$ (300 K)	$x = 0.05$ (300 K)	$x = 0.08$ (300 K)	$x = 0.1$ (300 K)	$x = 0.1$ (4 K)
Bond lengths (Å)					
Fe–O(1) × 2	1.998(4)	1.989(6)	1.983(8)	1.980(8)	2.017(2)
Fe–O(2) × 4	1.993(2)	1.988(3)	1.980(3)	1.978(3)	1.990(2)
Mo–O(1) × 2	1.952(4)	1.960(6)	1.965(8)	1.967(8)	1.933(2)
Mo–O(2) × 4	1.956(2)	1.962(3)	1.967(3)	1.968(3)	1.953(2)
Sr–O(1) × 4	2.786(0)	2.786(0)	2.786(0)	2.785(0)	2.777(0)
Sr–O(2) × 4	2.694(1)	2.697(2)	2.703(2)	2.708(2)	2.666(1)
Sr–O(2) × 4	2.889(1)	2.884(2)	2.877(2)	2.870(2)	2.910(1)
Fe–O(2)–Mo (deg)	171.99(7)	172.31(11)	172.87(13)	173.35(13)	169.92(7)
Bond valence sum (v.u.)					
Fe on Fe sites	3.17(1)	3.23(1)	3.29(2)	3.32(2)	
V on Fe sites	3.04(0)	3.09(1)	3.15(2)	3.18(2)	
Mo on Fe sites	4.73(1)	4.82(2)	4.91(3)	4.95(3)	
Fe on Mo sites	3.54(1)	3.48(2)	3.43(2)	3.42(2)	
V on Mo sites	3.39(1)	3.33(2)	3.28(2)	3.27(2)	
Mo on Mo sites	5.27(2)	5.19(2)	5.11(3)	5.10(3)	
Sr on Sr sites	2.00(0)	2.00(0)	2.00(0)	2.00(0)	
O on the 4*e* sites	2.06(1)	2.06(1)	2.06(2)	2.06(2)	
O on the 8*h* sites	2.07(0)	2.07(0)	2.06(0)	2.07(0)	
R_1	0.123	0.116	0.114	0.117	

Empirically, R_1 should be smaller than 0.2 v.u. for structures stable at room temperature [27]. For all the compounds investigated, the Global Instability Index R_1 is smaller than 0.13 v.u. at 300 K (Table 2), in contrast to the antisite model for the structure of A_2InNbO_6 (A = Ba, Sr) [26].

The bond lengths between the cations and oxygen shown in Table 2 reveal very slight distortions of the FeO_6 and MoO_6 octahedra at room temperature. The planar Fe–O–Mo angle increases slightly with the V content, indicating a reduction of the tetragonal distortion. However, the distortions are enhanced obviously at 4 K as reported for Sr_2FeMoO_6 and $Sr_2(Fe, T)MoO_6$ based on the NPD studies [15–17], manifesting the Fe t_{2g}–O p–Mo t_{2g} pdd–π interaction that is responsible for the double exchange mechanism [15]. For $Sr_2Fe_{0.9}V_{0.1}MoO_6$ at 4 K, the FeO_6 octahedra are elongated and the MoO_6 octahedra are compressed along the c direction (Table 2). Since the differences in charge and in cation size between Fe and Mo are comparable to those between V and Mo, the electronic effect is likely to be responsible for the selective occupation of V on the Mo sites in $Sr_2(Fe_{1-x}V_x)MoO_6$. Considering that the electron configuration of V^{3+} (t_{2g}^2) is close to that of Mo^{5+} (t_{2g}^1), it seems the cation with incomplete t_{2g} orbital favors a compressed octahedral environment. The recent work on $Sr_2Fe_{0.75}T_{0.25}MoO_6$ (T = Sc–Co) showed that the fraction of T on the Fe sites was significantly smaller for T = Ti, V and Co than for T = Sc, Mn and Fe [15], which seems to manifest the contribution of the electronic effect on the arrangement of B-site cations. As the V content increases, the distortion of the octahedra decreases and the electronic effect diminishes accordingly, then the V will occupy both the Fe and the Mo sites as reported for $Sr_2Fe_{0.75}V_{0.25}MoO_6$ [15]. This is in consistent with the trend that the difference between the bond valence sums on the Fe and the Mo sites of the 3d cation decreases with the V content.

High valence states of vanadium occur frequently in oxides, which might be an alternative origin of the selective substitution of V for Mo, because the ionic radii of V^{4+} and V^{5+} are smaller than that of Mo^{5+}. However, assuming V^{3+}, V^{4+} and V^{5+} on the Mo sites in $Sr_2Fe_{0.9}V_{0.1}MoO_6$, respectively, it is easy to check that the bond valence sum of the V ion would be 3.27, 3.65, and 3.85 v.u., i.e. the deviation from its assumed chemical valence would be 0.27, −0.35, and −1.15 v.u., and accordingly the Global Instability Index R_1 increases with the assumed chemical valence of V. The R_1 is increased by 45% for V^{5+}, which could result in destabilization of the structure.

The satisfactory agreements between the derived V content and the nominal composition, between the derived saturation magnetization and the experimental one, between the bond valence sum and the chemical valence, and the reasonably reproduced magnetization of the compounds as a function of the V content within the FIM model [14], all corroborate the refinement results.

5. Conclusions

Refinement of crystal and magnetic structure of $Sr_2(Fe_{1-x}V_x)MoO_6$ by alternately using XRD and NPD data at room temperature reveal that no oxygen deficiency exists and the V atoms selectively occupy the Mo sites for the V content up to $x = 0.1$. The AS content increases with

increasing V content. At room temperature the lattice distortion and the octahedra distortions decrease as the V content increases, whereas the distortions are enhanced obviously at low temperature. The magnetic structure models with the moments aligning along [001], [110] or [111] directions fit the NPD data of $Sr_2Fe_{0.9}V_{0.1}MoO_6$ at 4 K equally well. The later two models reproduce the total magnetic moment of the compound derived from magnetic measurement, whereas the [001] direction model results in a little smaller total magnetic moment than the experimental one.

Bond valence analysis based on the structure refinement results shows that Mo ions are compatible with both the Fe sites and the Mo sites. The bond valence sum of V is about 0.15 v.u. smaller than that of Fe on both the Fe and the Mo sites. At low doping level, the bond valence sum of the 3*d* cation is close to three on the Fe sites but obviously larger than three on the Mo sites. The difference between the bond valence sums on the Fe and the Mo sites of the 3*d* cation decreases with the V content. The selective occupation of the V on the Mo sites is likely due to the electronic effects because of the different distortions of the FeO_6 and MoO_6 octahedra. Therefore, the stability of double perovskites is controlled primarily by charge difference of the cations and secondarily by the size difference of the cations, but the contribution of configuration entropy due to the AS and that of the electronic effects should also be taken into account.

Acknowledgments

This work is supported by the National Natural Science Foundation of China, the State Key Project of Fundamental Research, and the exchange program between NIST and CAS.

References

[1] K.I. Kobayashi, T. Kimura, H. Sawada, K. Terakura, Y. Tokura, Nature (London) 395 (1998) 677.
[2] Y. Moritomo, Sh. Xu, A. Machida, T. Akimoto, E. Nishibori, M. Takata, M. Sakata, Phys. Rev. B 61 (2000) R7827.
[3] Y. Tomioka, T. Okuda, Y. Okimoto, R. Kumai, K.I. Kobayashi, Y. Tokura, Phys. Rev. B 61 (2000) 422.
[4] A. Maignan, C. Martin, M. Hervieu, B. Raveau, J. Magn. Magn. Mater. 211 (2000) 173.
[5] L.I. Balcells, J. Navarro, M. Bibes, A. Roig, B. Martinez, J. Fontcuberta, Appl. Phys. Lett. 78 (2001) 781.
[6] M.T. Anderson, K.B. Greenwood, G.A. Taylor, K.R. Poppelmeier, Prog. Solid State Chem. 22 (1993) 197.
[7] M. García-Hernández, J.L. Martínez, M.J. Martínez-Lope, M.T. Casais, J.A. Alonso, Phys. Rev. Lett. 86 (2001) 2443.
[8] A.S. Ogale, S.B. Ogale, R. Ramesh, T. Venkatesan, Appl. Phys. Lett. 75 (1999) 537.
[9] K.I. Kobayashi, T. Okuda, Y. Yomioka, T. Kimura, Y. Tokura, J. Magn. Magn. Mater. 218 (2000) 17.
[10] S. Ray, A. Kumar, S. Majumdar, E.V. Sampathkumaran, D.D. Sarma, J. Phys.: Condens. Matter 13 (2001) 607.
[11] C.L. Yuan, Y. Zhu, P.P. Ong, J. Appl. Phys. 91 (2002) 4421.
[12] X.M. Feng, G.H. Rao, G.Y. Liu, H.F. Yang, W.F. Liu, Z.W. Ouyang, L.T. Yang, Z.X. Liu, R.C. Yu, C.Q. Jin, J.K. Liang, J. Phys.: Condens. Matter 14 (2002) 12503.
[13] J. Blasco, C. Ritter, L. Morellon, P.A. Algarabel, J.M. De Tesera, D. Serrate, J. García, M.R. Ibarra, Solid State Sci. 4 (2002) 651.
[14] Q. Zhang, G.H. Rao, X.M. Feng, G.Y. Liu, Y.G. Xiao, Y. Zhang, J.K. Liang, Solid State Commun. 133 (2005) 223.
[15] C. Ritter, J. Blasco, J.M. De Teresa, D. Serrate, L. Morellon, J. García, M.R. Ibarra, Solid State Sci. 6 (2004) 419.
[16] O. Chmaissem, R. Kruk, B. Dabrowski, D.E. Brown, X. Xiong, S. Kolesnik, J.D. Jorgensen, C.W. Kimball, Phys. Rev. B 62 (2000) 14197.
[17] C. Ritter, M.R. Ibarra, L. Morellon, J. Blasco, J. García, J.M. De Teresa, J. Phys.: Condens. Matter 12 (2002) 8295.
[18] D. Sánchez, J.A. Alonso, M. García-Hernández, M.J. Martínez-Lope, J.L. Martínez, A. Mellergård, Phys. Rev. B 65 (2002) 104426.
[19] J. Rodríguez-Carvajal, Physica B 192 (1993) 55.
[20] M.W. Lufaso, P.M. Woodward, Acta Crystallogr. B 60 (2004) 10.
[21] A. Williams, G.H. Kwei, A.T. Ortiz, M. Karnowski, W.K. Warburton, J. Mater. Res. 5 (1990) 1197.
[22] L.B. McCusker, R.B. Von Dreele, D.E. Cox, D. Louër, P. Scardi, J. Appl. Crystallogr. 32 (1999) 36.
[23] Q. Zhang, G.Y. Liu, G.H. Rao, Solid State Commun. 138 (2006) 294.
[24] W.T. Fu, D. Visser, D.J.W. Ijdo, Solid State Commun. 134 (2005) 647.
[25] V. Ting, Y. Liu, R.L. Withers, L. Norén, M. James, J.D. Fitz Gerald, J. Solid State Chem. 179 (2006) 551.
[26] R.D. Shannon, Acta Crystallogr. A 32 (1976) 751.
[27] I.D. Brown, Acta Crystallogr. B 48 (1992) 553.
[28] A. Guinier, X-ray Diffraction in Crystals, Imperfect Crystals and Amorphous Bodies, W.H. Freeman & Company, San Franisco, London, 1963.